https://doi.org/10.1093/plphys/kiad031 PLANT PHYSIOLOGY 2023: 191: 2276–2287

Plant Physiology®

Research Article

Overexpressing *Vitamin C Defective 2* reduces fertility and alters Ca^{2+} signals in Arabidopsis pollen

Chrystle Weigand,[1] **Deborah Brady**,[1] **James A. Davis**,[1] **Tori Speicher**,[1] **Jonathan Bacalso**,[1] **Dylan Jones**,[1] **Gad Miller**,[2] **Won-Gyu Choi**[1] **and Jeffrey F. Harper**[1,*]

1 Department of Biochemistry and Molecular Biology, University of Nevada, Reno, Nevada 89557, USA
2 Department of Plant Sciences, The Mina and Everard Goodman Faculty of Life Sciences Bar Ilan University, Ramat-Gan 5290002, Israel

*Author for correspondence: jfharper@unr.edu (J.F.H.)

C.W. authored the manuscript and contributed the following: mRNA expression analyses, pollen tube growth and morphology, ascorbate analysis, ROS microscopy and analyses, calcium microscopy and analyses, expression profiling, and genetics for empty vector controls. D.B. and C.W. performed genetic analyses, pollen germination events, and identified homozygous lines. T.S. isolated ascorbate from pollen and conducted an ascorbate assay. J.A.D., J.B., and D.J. were involved in the collection, microscopy, and analysis of the seed set. G.M. and W.-G.C. helped design and interpret experiments. J.F.H. performed plant crosses, cloned plasmid constructs, and supervised the research. J.F.H. and J.A.D. also assisted C.W. in writing. J.F.H. agrees to serve as the author responsible for contact.
The author responsible for distribution of materials integral to the findings presented in this article in accordance with the policy described in the Instructions for Authors (https://academic.oup.com/plphys/pages/General-Instructions) is Jeffrey F. Harper (jfharper@unr.edu).

Abstract

A potential strategy to mitigate oxidative damage in plants is to increase the abundance of antioxidants, such as ascorbate (i.e. vitamin C). In Arabidopsis (*A. thaliana*), a rate-limiting step in ascorbate biosynthesis is a phosphorylase encoded by *Vitamin C Defective 2* (*VTC2*). To specifically overexpress *VTC2* (*VTC2* OE) in pollen, the coding region was expressed using a promoter from a gene with ~150-fold higher expression in pollen, leading to pollen grains with an eight-fold increased *VTC2* mRNA. *VTC2* OE resulted in a near-sterile phenotype with a 50-fold decrease in pollen transmission efficiency and a five-fold reduction in the number of seeds per silique. In vitro assays revealed pollen grains were more prone to bursting (greater than two-fold) or produced shorter, morphologically abnormal pollen tubes. The inclusion of a genetically encoded Ca^{2+} reporter, mCherry-GCaMP6fast (CGf), revealed pollen tubes with altered tip-focused Ca^{2+} dynamics and increased bursting frequency during periods of oscillatory and arrested growth. Despite these phenotypes, *VTC2* OE pollen failed to show expected increases in ascorbate or reductions in reactive oxygen species, as measured using a redox-sensitive dye or a roGFP2. However, mRNA expression analyses revealed greater than two-fold reductions in mRNA encoding two enzymes critical to biosynthetic pathways related to cell walls or glyco-modifications of lipids and proteins: GDP-D-mannose pyrophosphorylase (GMP) and GDP-D-mannose 3′,5′ epimerase (GME). These results support a model in which the near-sterile defects resulting from *VTC2* OE in pollen are associated with feedback mechanisms that can alter one or more signaling or metabolic pathways critical to pollen tube growth and fertility.

Introduction

Increasing antioxidant production in crop plants is a potential strategy to mitigate toxic increases in reactive oxygen species (ROS) arising from abiotic stress (Kerchev and Van Breusegem, 2022). In vivo, hydrogen peroxide (H_2O_2; $t_{1/2} >$ 1 ms) is a relatively stable form of ROS that can be transported across membranes, whereas superoxide (O_2^-; $t_{1/2}$ ~1–4 μs) and hydroxyl radicals ($^{\bullet}OH$; $t_{1/2}$ ~ 1 ns) are more unstable. This wider distribution of H_2O_2 increases the potential for widespread oxidation of lipids, proteins, and DNA (Mittler, 2017). To prevent oxidative damage, plants generate a wide array of antioxidants to quench ROS (Shao et al.,2008; Laxa et al.,2019), one of which is ascorbate (Figure 1) (Foyer and Noctor, 2011; Smirnoff, 2018).

Received July 19, 2022. Accepted December 21, 2022. Advance access publication January 27, 2023
© American Society of Plant Biologists 2023. All rights reserved. For permissions, please e-mail: journals.permissions@oup.com

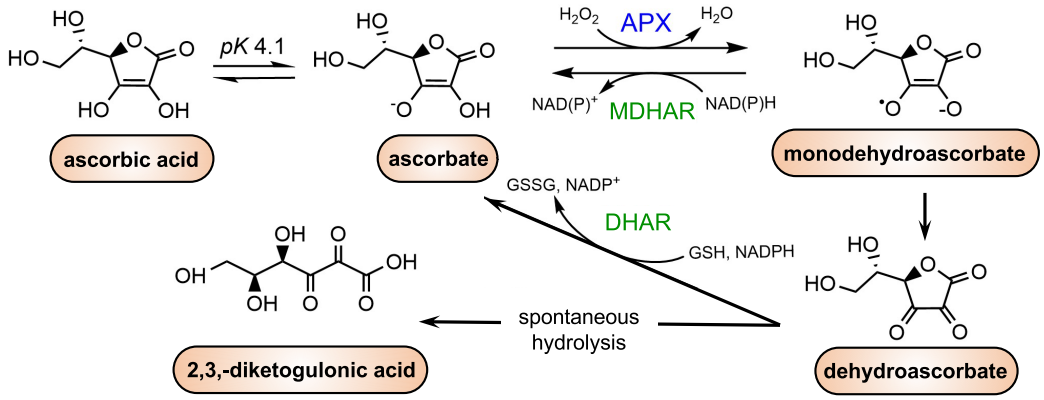

Figure 1 Ascorbate (vitamin C) metabolism in plants. Ascorbate quenches hydrogen peroxide (H_2O_2) to form H_2O by electron transfer via ascorbate peroxidase (APX), resulting in monodehydroascorbate (MDHA). MDHA undergoes further oxidation by ROS to dehydroascorbate (DHAR). MDHA and DHA can be recycled back to ascorbic acid via MDHA reductase (MDHAR) and DHA reductase (DHAR), respectively, and NAD(P)H and glutathione cofactors. Spontaneous hydrolysis irreversibly converts DHA to 2,3-diketogulonic acid (Smirnoff, 2018; Hasanuzzaman et al., 2019).

Ascorbate (i.e. vitamin C) is one of the most abundant antioxidants in plant cells, ranging from nanomolar to millimolar concentrations throughout the cell. Ascorbate is transported into organelles and the extracellular matrix (i.e. apoplast), where it can undergo oxidation to monodehydroascorbate (MDHA) or dehydroascorbate (DHA) and then recycle back to ascorbate via MDHA reductase and DHA reductase using NAD(P)H or reduced glutathione as cofactors (Figure 1) (Gallie, 2012; Smirnoff, 2018; Hasanuzzaman et al., 2019). However, if DHA is spontaneously hydrolyzed to 2,3-diketogulonic acid, a subsequent oxidation step can occur, resulting in an unknown intermediate reported to increase H_2O_2 production (Hasanuzzaman et al., 2019). Similarly, ascorbate itself can become a pro-oxidant by participating in the production of free radicals via Fenton reactions (Smirnoff, 2018). Despite ascorbate's potential role as both a pro- and anti-oxidant, its high redox potential generally favors its function in mitigating toxic ROS levels during oxidative stress.

Although there are three distinct routes to ascorbate production in the Smirnoff–Wheeler pathway, ascorbate biosynthesis via the GDP-L-galactose branch is considered dominant (Figure 2) (Fenech et al., 2019). A precursor to this GDP-L-galactose branch is the conversion of D-mannose-1-P to GDP-D-mannose, where GDP-D-mannose is a central branching point between ascorbate production, synthesis of cell wall polysaccharides, and carbohydrate metabolism (Qi et al., 2017). After GDP-D-mannose is converted to GDP-L-galactose, an important rate-limiting step is the subsequent conversion of GDP-L-galactose to galactose-1-phosphate via a phosphorylase encoded by the gene *Vitamin C Defective 2* (*VTC2*) (Gao et al., 2011; Yoshimura et al., 2014). The *VTC2*-encoded phosphorylase is also regulated at the translational level through an upstream open reading frame (uORF), where the overaccumulation of ascorbate provides negative feedback to decrease the abundance of VTC2 (Laing et al., 2015).

The overexpression of *VTC2*, via promoter swapping or editing *VTC2*'s uORF, was reported to increase ascorbate production in leaves, thereby improving plant tolerance to abiotic stress (Bulley et al., 2012; Wang et al., 2014; Zhang et al., 2020). While previous studies associated increased ascorbate with smaller fruits and fewer seeds in tomato (*Solanum lycopersicum*) (Bulley et al., 2012), only recently was the overexpression of *VTC2* linked to reduced pollen germination (Deslous et al., 2021). Although an increase in pollen ascorbate was not directly confirmed, the reduced pollen germination was speculated to arise from a disruption in redox-dependent events in pollen development, raising a doubt as to whether increasing ascorbate levels in pollen is a viable strategy to improve pollen thermotolerance. In this study, we provide evidence that *VTC2* overexpression in Arabidopsis (*A. thaliana*) pollen severely reduced pollen fertility without showing a significant increase in the accumulation of ascorbate, or changes in the redox potential of the pollen grain cytoplasm. This underscores the need to consider alternative scenarios in which *VTC2* overexpression might increase or decrease the flux of metabolites into other pathways, such as cell wall biogenesis or glycosylation of proteins or lipids. Interestingly, *VTC2* overexpression altered calcium (Ca^{2+}) signaling dynamics associated with growing pollen tubes, with an increase in the average magnitude of tip-focused Ca^{2+} oscillations during oscillatory growth, as well as the absence of distinct oscillations during periods of arrested growth. While it is not yet clear whether these changes in Ca^{2+} dynamics are the cause or consequence of *VTC2*-dependent pollen infertility, they invite speculation on the mechanistic relationship between Ca^{2+} signaling and the metabolic pathways related to vitamin C production.

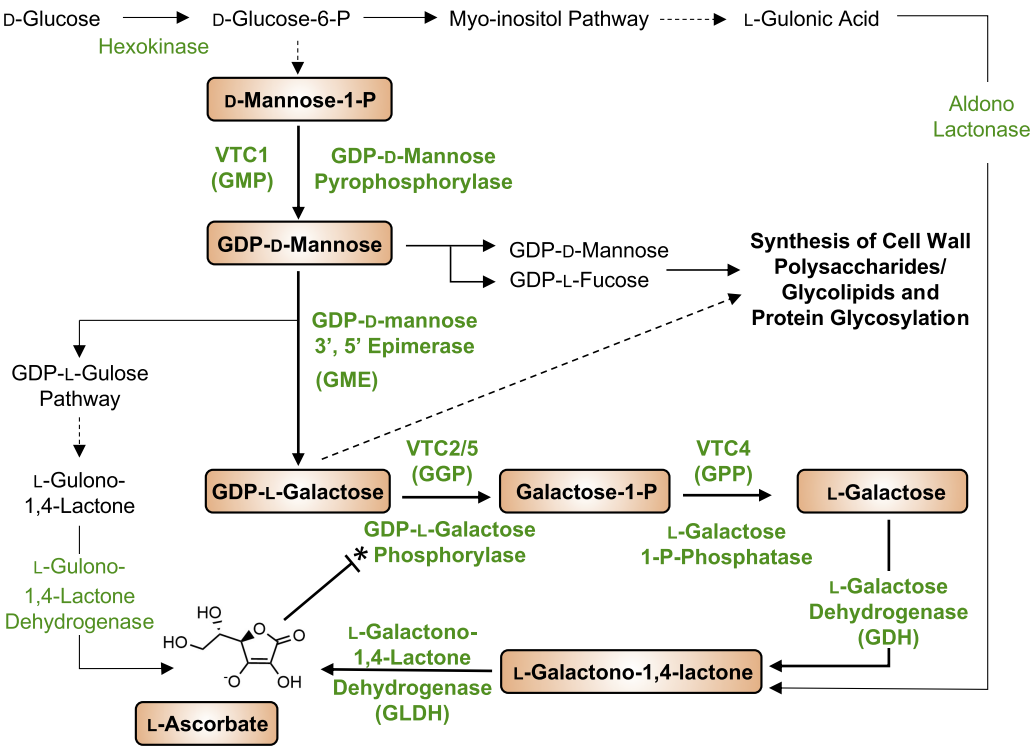

Figure 2 Ascorbate biosynthesis via the Smirnoff–Wheeler pathway. Ascorbate biosynthesis occurs through three pathways: L-Galactose, L-Gulose, and *Myo*-inositol pathways. Solid arrows are direct steps. Dashed arrows represent several enzymatic or non-enzymatic steps. Enzymes are shown in green with respective abbreviations or alternative nomenclature (i.e. GDP-D-mannose pyrophosphorylase (GMP) is also Vitamin C Defective 1 (VTC1)). Substrates of interest are beige. Bold, solid arrows indicate the L-Galactose pathway. Arrows replaced with lines represent inhibition. *Elevated ascorbate levels lead to the translation of *VTC2*'s upstream ORF, resulting in translational inhibition of VTC2. (Gao et al., 2011; Laing et al., 2015; Qi et al., 2017; Tao et al., 2018).

Results

VTC2 overexpression reduces seed set and pollen fertility

To determine whether *VTC2* overexpression in pollen directly affects male fertility, a transgene encoding VTC2 under the control of a pollen-dominant promoter (upstream region of *Ca^{2+}-dependent Protein Kinase 34*, *At5g19360*) was introduced into wild-type (WT) Col-0. This promoter was chosen because *CPK34* is expressed more than 150-fold higher in pollen relative to female or vegetative tissues (Supplemental Figure S1). Thus, the *CPK34p::VTC2* transgene was designed to selectively increase *VTC2* expression in pollen, leaving other non-pollen tissues with normal endogenous *VTC2* expression. For two representative lines used here, a greater than 8-fold overexpression (OE) of *VTC2* was confirmed in pollen grains using reverse transcription-quantitative polymerase chain reaction (RT-qPCR) (Figure 3B and Supplemental Figure S1).

To test for impacts of *VTC2* OE in pollen, plants heterozygous for the *VTC2* transgene were tested for a segregation distortion phenotype. The transmission efficiency (TE) of the transgene was scored in F1 progeny by counting hygromycin-resistant (Hyg^R) and sensitive seedlings (Figure 3A). In the case of OE1 and OE2 plants that were allowed to self-pollinate, the TE ratio dropped from the expected ratio of 3:1 to ~1:1 ($P < 0.001$). Reciprocal crosses indicated that transmission through the ovule (i.e. female) was normal (~50% TE; $P > 0.6$), whereas transmission through pollen (i.e. male) was reduced ~50-fold (~1% TE; $P < 0.001$). This pollen-specific infertility was observed in all 20 independent transgenic lines examined. Vector controls showed no segregation distortions through male or female gametes (Supplemental Figure S2).

Two additional studies were performed to further understand how *VTC2* OE impacted pollen fertility. First, to address whether the ~50-fold decrease in pollen TE was simply due to slower pollen tube growth, a limited pollination outcross (fewer pollen than ovules) was performed. A limited pollen assay provides an equal opportunity for slow pollen to fertilize ovules (Weigand and Harper, 2020) and thus, potentially restore normal transmission frequencies for *VTC2* OE pollen. Nevertheless, pollen transmission did not improve under limited pollination conditions, indicating fertility defects associated with *VTC2* OE were not simply caused by slower-growing pollen tubes (Figure 3A).

Second, to investigate whether *VTC2* OE might still render a protective effect on pollen fertility during a potential ROS-elevating stress, self-pollination and pollen outcrosses were performed under hot/cold stress conditions

A

Male x Female	Condition	Total *n* line 1, 2	Exp TE (%)	Obs TE (%) line 1, 2	*p*-value (sum)
Self *CPK34p::VTC2*	Normal	147,150	75	54,55	<0.001
	Hot/ Cold Stress	288,548	75	58,52	<0.001
COL-0 x *CPK34p::VTC2*	Normal	114,67	50	45,49	>0.6
CPK34p::VTC2 x *ms1*	Normal	433,253	50	1,0	<0.001
	Limited Pollination	203,112	50	3,0	<0.001
	Hot/ Cold Stress	114,152	50	1,5	<0.001
Vector Control x *ms1*	Normal	264, 286	50	55,48	>0.6

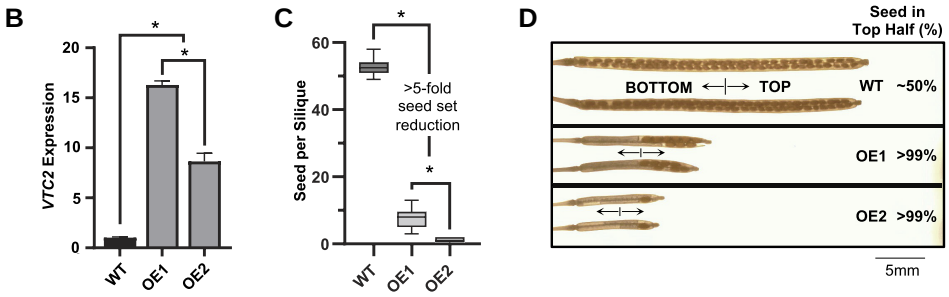

Figure 3 *VTC2* OE reduces seed set and pollen fertility. A, Genetic crosses showing reduced pollen transmission of a transgene expressing *VTC2* under the control of a pollen-specific promoter from *AtCPK34* (*CPK34p::VTC2*, ps3059). Progeny of selfed plants and reciprocal outcrosses were scored for transmission efficiency (TE) of a heterozygous hygromycin resistant transgene. TE = # resistant seedlings/total # seedlings. Statistical significance was determined by Pearson's Chi-square test (χ^2) with a minimum threshold set at $P < 0.05$. Total *n*, obs TE%, and *P*-values are shown for overexpression (OE) line 1 (left, ss2695) and OE2 (right, ss2696). B, *CPK34p::VTC2* increases *VTC2* mRNA abundance in pollen, shown by RT-qPCR of *VTC2* in comparison to a reference gene *Cyclin P2; 1*. Error bars represent ± S.E.M., $n = 3$ biological replicates analyzed in duplicate. Asterisk indicates significance determined by Student's *t*-test, $P < 0.00001$. C and D, *VTC2* OE reduces seed set, as shown by (C) quantification of average seed numbers per silique and (D) pattern of seed deposition (% seed in the top half), shown by cleared siliques, between WT and homozygous OE lines (OE1 ss2697and OE2 ss2698). Boxplot elements include a median (center line), interquartile range (inside box), and S.E.M. (whiskers), $n = 10$. Asterisk indicates significance determined by Student's *t*-test, $P < 0.00001$. See Supplemental Figures S1 and S2 for expression details and genetics for vector control, respectively.

(Rahmati Ishka et al., 2018). To create a stress regime with hot days and cold nights, temperature conditions cycled between −1°C and 40°C (Tunc-Ozdemir et al., 2013). However, there was no indication of improved transmission for pollen harboring the *VTC2* OE transgene under this temperature stress environment (Figure 3A).

Although *VTC2* OE reduced pollen transmission, it was still possible to generate plants homozygous for the *CPK34p::VTC2* transgene. The seed set for homozygous lines OE1 and OE2 was reduced more than 5-fold compared to WT plants grown in parallel (Figure 3, C and D). Together, these results support the contention that pollen-specific increases in *VTC2* expression result in pollen-autonomous fertility defects.

VTC2 OE resulted in pollen germination and tube growth defects

To identify potential pollen defects, pollen were subjected to in vitro germination and pollen tube growth assays. Compared to WT, pollen grains from homozygous OE lines 1 and 2 showed a ~2-fold increase in the frequency of bursting at the time of germination (Figure 4A). Among grains that formed tubes, the average tube length was more than 2-fold shorter (Figure 4B). An in vivo confirmation of this short pollen phenotype was supported by the observation that more than 99% of the fertilization events occurred in the upper half of the silique (i.e. nearest the stigma end of the pistil) (Figure 3D).

In WT pollen tubes, it is common to observe some variation in tube width and morphologies. However, OE pollen tubes showed more than a 2-fold greater variation between the widest and narrowest regions of the tube (Figure 4, C and D). Together, these results suggest that deficiencies in germination and tube growth could account for at least some of the pollen fertility defects associated with *VTC2* OE.

VTC2 OE failed to elevate concentrations of ascorbate in pollen grains

To determine if *VTC2* overexpression lines produced pollen grains with higher levels of ascorbate, a fluorometric method was used to quantify ascorbate concentrations. Ascorbate was quantified by assaying the fluorescence of 3-(dihydroxyethyl)furo[3,4-b]quinoxaline-1-one, the product of a two-step hydroxylamine oxidation–condensation reaction that

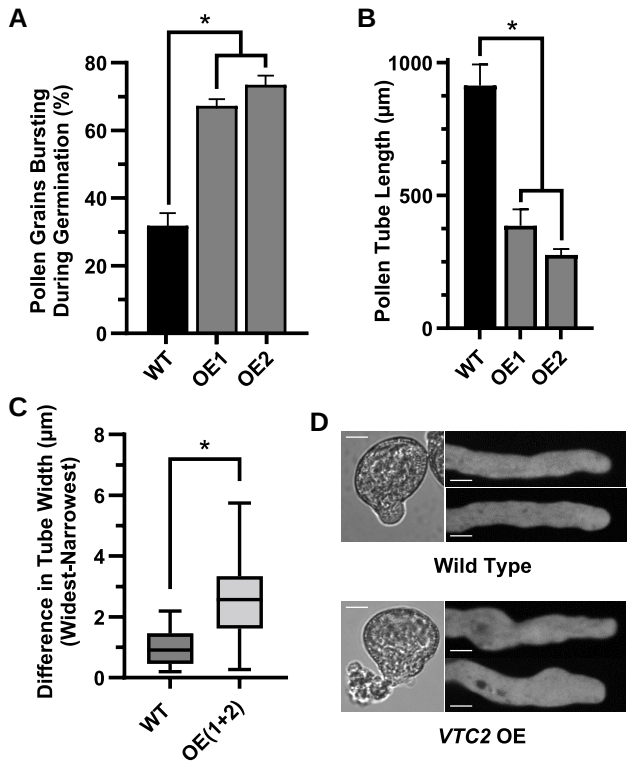

Figure 4 *VTC2* OE pollen develop fewer and shorter pollen tubes compared to WT. A, Pollen grain bursting events during germination. Error bars represent ± S.E.M., Col-0, $n = 250$; OE L1, $n = 540$; OE L2, $n = 740$. The asterisk indicates significance by Pearson's Chi-square test (χ^2), df = 1, $P < 0.001$. B, Pollen tube length between WT and OE VTC2 (after 10 h) grown in vitro on agar solidified media. Error bars represent ± S.E.M., $n = 30$. Asterisk indicates significance by one-way ANOVA and Tukey test, $P < 0.0001$. Data were collected from homozygous plants harboring *CPK34p::VTC2* (ps3059, OE1 ss2697, and OE2 ss2698). C, Quantification of differences in tube width. Boxplot elements include a median (center line), interquartile range (inside box), and S.E.M. (whiskers), $n = 30$. The asterisk indicates significance by Student's *t*-test, $P < 0.001$. D, Pictures of grain bursting and abnormal tube morphologies in *VTC2* OE pollen. Scale bar = 5 µm.

directly corresponds with ascorbate concentrations (Vislisel et al., 2007). While *VTC2* OE lines displayed a trend toward lower ascorbate (1.3-fold), this difference was not significant ($P > 0.05$) (Figure 5A) and was within the range of reported ascorbate concentrations in Arabidopsis seedlings (Müller-Moulé, 2008) and tomato fruits (Deslous et al., 2021). A failure to detect increased ascorbate suggests that fertility defects in the *VTC2* OE lines were not caused by increases in the steady-state concentrations of ascorbate.

VTC2 OE failed to reduce ROS levels in mature pollen grains

Despite the failure to detect *VTC2*-dependent increases in ascorbate, two different assays were still used to evaluate whether redox homeostasis might have been impacted. In the first assay, the relative redox potential of pollen grains was evaluated using 2′-7′-dichlorodihydrofluorescein diacetate (DCF), a fluorescent stain that increases intensity as it undergoes oxidation by ROS (Luria et al., 2019). To provide a control for plant-to-plant variation and environmental variables, pollen grains were analyzed from plants segregating a transgene construct harboring both *VTC2* and an ER-mCherry visualization marker targeted to the endoplasmic reticulum (ER) (*CPK34p::VTC2* and *CPK34p::ER-mCherry*). Fluorescence from the ER-mCherry allowed the transgenic pollen to be identified and directly compared to WT pollen produced by the same parental plant. In pollen from plants heterozygous for OE1 or OE2, there was no significant difference observed for DCF fluorescence between WT and *VTC2* OE pollen (Figure 5B). As an independent method, pollen grains were evaluated using a roGFP2 as a genetically encoded redox-sensitive ratiometric reporter (Ugalde et al., 2020). To determine the redox state of roGFP2, pollen from plants expressing either *UBQ10p::mCherry-roGFP2* (WT + reporter) or co-expressing *CPK34p::VTC2* and *UBQ10p::mCherry-roGFP2* (OE + reporter) were imaged for the relative intensity of the 520 nm emission peak resulting from an excitation at either 405 nm (higher in the oxidized state) or 488 nm (higher in the reduced state). Compared to WT, the roGFP2 excitation ratios for *VTC2* OE lines indicated a slightly more oxidized cytosolic environment (i.e. less, rather than more "ROS quenching") ($P < 0.0001$) (Figure 5C). Taken together with the DCF staining assay, our results indicate that *VTC2* OE failed to generate a less oxidized redox status compared to WT.

VTC2 OE alters tip-focused Ca^{2+} signaling in pollen tubes

Because tip-focused Ca^{2+} oscillations are proposed to be essential to polarized pollen tube growth (Frietsch et al., 2007; Johnson et al., 2019), a ratiometric Ca^{2+} reporter mCherry-GCaMP6fast (CGf) from Weigand et al. (2021) was used to investigate whether *VTC2* OE altered Ca^{2+} dynamics. There are three main growth-related Ca^{2+} signaling patterns that have been reported for pollen tubes: steady-, oscillatory-, and arrested-growth Ca^{2+} oscillations (i.e. SGC, OGC, and AGC oscillations, respectively) (Damineli et al., 2017; Weigand et al., 2021). For pollen tubes that displayed SGC oscillations, there were no obvious differences in oscillations between WT and *VTC2* OE lines (Figure 6, A and B). However, major differences were observed during periods of both OGC and AGC oscillations.

During oscillatory growth, WT pollen exhibited a classical pattern of growth cycles followed by Ca^{2+} oscillations (OGC oscillations), as shown by synchronized peaks between CGf ratios (black) and growth rates (green) (Figure 6C, left). In contrast, OE pollen displayed WT-like OGC oscillations (Figure 6C, right) but with significantly higher peak Ca^{2+} (i.e. CGf) ratios and larger amplitude changes (Figure 6, D and E) ($P < 0.001$).

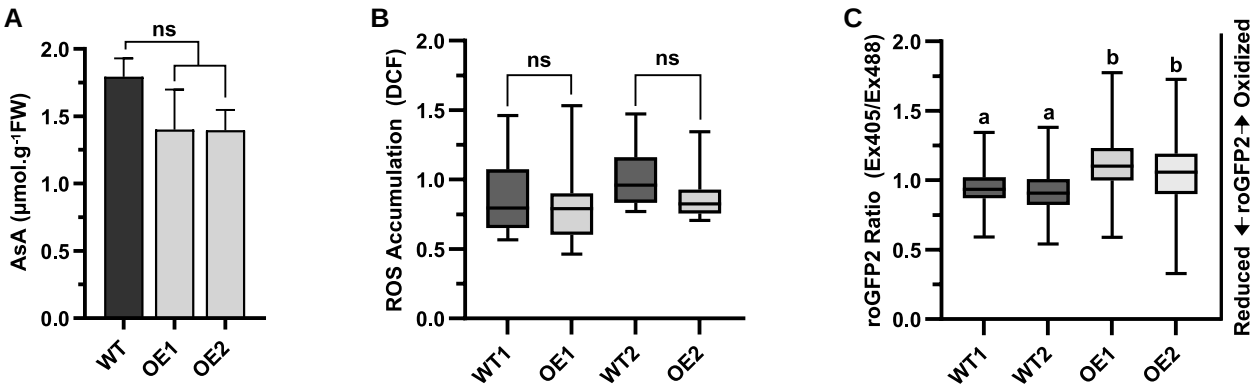

Figure 5 *VTC2* OE does not increase ascorbate or lower redox potential in mature pollen grains. A, Spectrophotometric assay for the abundance of ascorbate (AsA) in the pollen of two lines homozygous for *CPK34p::VTC2* (ps3059: OE1 ss2697, and OE2 ss2698). Error bars represent ± S.E.M., $n = 6$. B, ROS accumulation detected by 2′-7′-Dichlorodihydrofluorescein diacetate (H_2DCFDA, DCF). WT and transgenic pollen grains produced from the same flower of heterozygous plants were compared by scoring for the OE pollen that showed coexpression of an ER-localized mCherry (ps3059, OE1 ss2695, and OE2 ss2696). Boxplot elements include a median (center line), interquartile range (inside box), and S.E.M. (whiskers), $n = 20$. C, Redox state of roGFP2 in pollen grains. Results are shown using two independent transgenic lines for each genotype. Boxplot elements include a median (center line), interquartile range (inside box), and S.E.M. (whiskers), $n = 550$. Statistical significance was determined using one-way ANOVA and Tukey test with minimum threshold of $P < 0.01$. ns = not significant. "a" and "b' = significantly different means. WT with *UBQ10p::mCherry-roGFP2* (ps3209, WT1 ss2673 and WT2 ss2674). *VTC2 OE* with *UBQ10p::mCherry-roGFP2* (ps3217, OE1 ss2676 and OE2 ss2677).

During arrested growth, WT pollen displayed typical AGC oscillations with distinct intervals between very high peaks and very low valleys (Figure 6F, left). In contrast, OE pollen showed a reduction in peak magnitudes (Figure 6, F right and G) and the loss of distinct repeating intervals (Figure 6H) ($P < 0.0001$).

VTC2 OE reduces *GMP* and *GME* mRNA expression levels

To determine if *VTC2* OE altered the expression for genes encoding key enzymes upstream of VTC2 (Figure 7), RT-qPCR analyses were performed to quantify the relative abundance of mRNA encoding GDP-D-mannose pyrophosphorylase (GMP) and GDP-D-mannose 3′,5′ epimerase (GME). In homozygous OE lines, *GMP* mRNA expression was reduced 2-fold in OE1 and 4-fold in OE2 ($P < 0.0001$). Similarly, *GME* expression was reduced 1.5-fold in OE1 and 2-fold in OE2 ($P < 0.01$). Together, reductions in *GMP* and *GME* expression suggest that *VTC2* OE results in feedback regulation of genes corresponding to at least two of the upstream biosynthetic steps (Figure 2) that could impact multiple pathways linked to carbohydrate-related modifications of lipids, proteins, or cell walls.

Discussion

Increasing the production of vitamin C in plants has potential benefits for both nutritional fortification and improved stress tolerance (Kerchev and Van Breusegem, 2022). A rate-limiting step in ascorbate biosynthesis is the conversion of GDP-L-galactose to galactose-1-phosphate via a phosphorylase encoded by a gene named *VTC2* (Yoshimura et al., 2014). *VTC2* overexpression constructs have been stably expressed in a wide variety of crops including tomato (*Solanum lycopersicum*) (Deslous et al., 2021), tobacco (*Nicotiana tabacum*) (Wang et al., 2014), strawberry (*Fragaria* x *ananassa*), and potato (*Solanum tuberosum*) (Bulley et al., 2012), with each study resulting in increased ascorbate and in some cases improved stress tolerance. However, impaired seed development was also noted in tomato plants overexpressing *VTC2* using a transgene driven by *35S* promoter (Bulley et al., 2012) or by a clustered regularly interspaced short palindromic repeats (CRISPR)-edited endogenous *VTC2* uORF (Deslous et al., 2021).

Here in Arabidopsis, we show a similar reproductive deficiency when *VTC2* is overexpressed using a transgene with a pollen-specific promoter. In this study, a *CPK34p::VTC2* transgene was introduced into WT Arabidopsis, resulting in a nearly 50-fold decrease in pollen transmission and, in homozygous transgenic plants, a more than 5-fold decrease in the number of seeds per silique. This indicates that *VTC2* OE can result in a pollen autonomous defect that dramatically reduces reproductive fertility and seed production in Arabidopsis. Importantly, the observed decrease in pollen fertility remained unchanged under hot/cold stress conditions (Figure 3), suggesting that *VTC2* OE in pollen did not provide any significant benefits for improving reproductive stress tolerance.

Reduced pollen transmission is caused by fewer and shorter tubes

Multiple lines of evidence indicate that the *VTC2* OE fertility defects were primarily due to fewer and shorter pollen tubes, and not a decrease in pollen tube growth rates. First, when there was no competition between slow- and fast-growing pollen (i.e. limited pollen assays) (Weigand and Harper, 2020), the transmission efficiencies of *VTC2* OE pollen remained low (Figure 3). Thus, the segregation distortion

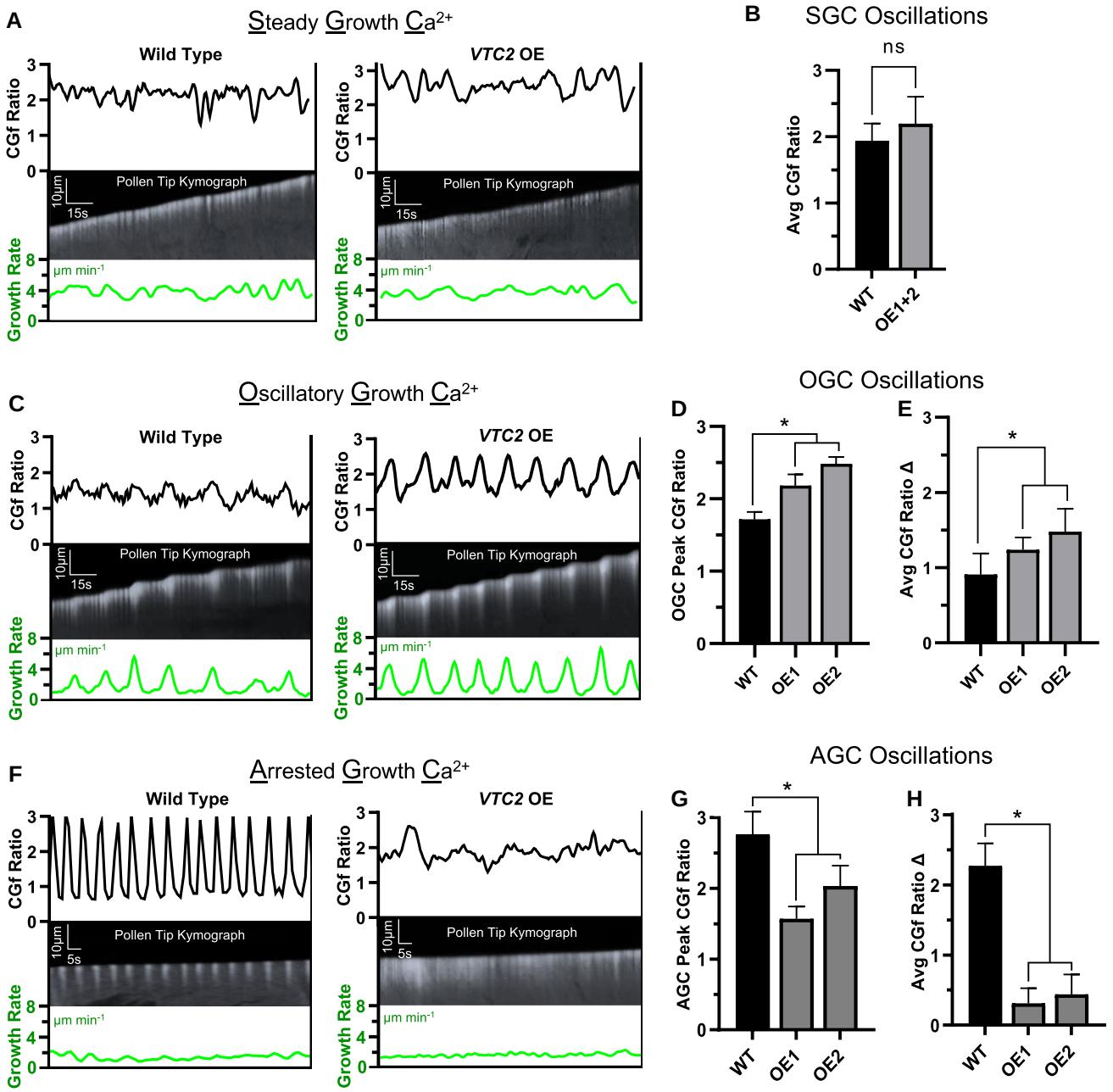

Figure 6 *VTC2* OE alters tip-focused $[Ca^{2+}]_{cyt}$ oscillations in pollen tubes. A, Comparison of steady growth Ca^{2+} (SGC) oscillations, shown by CGf ratio (black) and growth rate (green) between WT (left) and *VTC2* OE (right) pollen tubes. B, Average CGf ratio during steady growth ($n = 9$). C, Comparison of oscillatory growth Ca^{2+} (OGC) oscillations, followed by (D) peak CGf ratio and (E) average CGf ratio change (Δ) during oscillatory growth ($n = 12$). F, Comparison of arrested growth Ca^{2+} (AGC) oscillations, followed by (G) peak CGf ratio and (H) average CGf ratio change (Δ) during arrested growth ($n = 12$). Error bars represent ± S.E.M. Asterisk indicates significance by Pearson's Chi-square test ($\chi 2$) (Figure 4B) or one-way ANOVA and Tukey test, $P < 0.05$. WT with *CGf* (ps2935, WT1 ss2540, WT2 ss2640). *VTC2 OE* with CGf (ps3202, OE1 ss2709, and OE2 ss2710). Scale bar (A, C) 10 μm and 15 s and (F) 10 μm and 5 s.

observed with *VTC2* OE pollen cannot be explained by a simple decrease in pollen fitness due to slower-growing pollen tubes. Second, *VTC2* OE pollen tubes were 2-fold shorter than WT in vitro (Figure 4B). A short pollen phenotype was also supported by in vivo evidence of seed deposition patterns, where *VTC2* OE pollen fertilized ovules nearest the stigma end of the pistil (Figure 3D). Lastly, OE lines showed a 2-fold increase in pollen grain bursting when germinated in vitro (Figure 4A). A germination defect was also observed in tomato pollen from a plant harboring a CRISPR-edited *VTC2*'s uORF (Deslous et al., 2021).

The similarities between *VTC2* OE in tomato and Arabidopsis, such as reduced seed set and pollen germination defects, suggest that *VTC2* OE can cause or contribute to

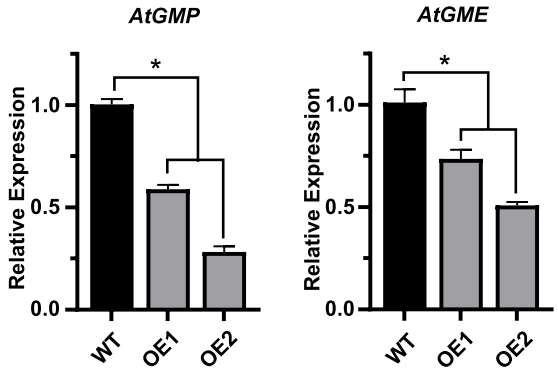

Figure 7 *VTC2* OE reduces *GMP* and *GME* expression levels in pollen grains. Relative quantitative expression of (left) *GMP* and (right) *GME* between WT and *VTC2* overexpression lines (OE1 ss2697and OE2 ss2698). Error bars represent ± S.E.M., $n = 3$ biological replicates analyzed in duplicate. The asterisk indicates significance by Student's *t*-test, $P < 0.05$.

pollen autonomous defects across multiple angiosperms. However, one important difference is that the tomato experiments potentially altered *VTC2* ubiquitously and might have impacted other aspects of plant development or reproduction, whereas Arabidopsis experiments here utilized a pollen-specific promoter to minimize secondary impacts from non-pollen tissues. Although it is unclear if pollen defects are the sole cause of reduced fertility in tomatoes, future studies are still warranted to determine if *VTC2* OE in female reproductive tissues can positively or negatively impact fertility.

Pollen defects did not correspond with an increase in ascorbate or a decrease in ROS

Despite expectations, experiments here failed to provide evidence that *VTC2* OE resulted in a measurable increase in pollen ascorbate concentrations or a subsequent decrease in ROS resulting from higher antioxidant levels (Figure 5). Previous *VTC2* OE studies observed measurable increases in ascorbate concentrations (3- to 6-fold in tomatoes and 2-fold in strawberries) (Bulley et al., 2012). However, those studies were not designed to specifically increase *VTC2* OE during pollen development, and, in the case of Deslous et al. (2021), increased amounts of ascorbate were only measured in the context of the entire flower and not specifically in pollen. As such, future studies are needed to elucidate if ascorbate biosynthesis or steady-state concentrations might be regulated differently in pollen compared to other tissues or between different angiosperms, such as tomato and Arabidopsis. Regardless, two different assays (DCF staining and roGFP2 imaging) failed to provide any evidence for a potential *VTC2*-triggered increase in antioxidant activities (Figure 5, B and C).

VTC2 OE disrupts OGC and AGC Ca^{2+} signaling in pollen tubes

Because *VTC2* OE pollen tubes exhibited growth deficiencies and abnormalities in morphology, we investigated whether *VTC2* OE could change growth-associated Ca^{2+} signals using a Ca^{2+} reporter (CGf) (Weigand et al., 2021). The evidence here indicates that *VTC2* OE altered Ca^{2+} oscillation patterns during oscillatory and arrested growth (i.e. OGC and AGC), whereas steady growth signals were relatively normal (Figure 6). More specifically, OGC oscillations in *VTC2* OE lines displayed higher peak Ca^{2+} ratios and larger amplitude changes, and AGC oscillations had reduced peak magnitudes and a loss of interval repeats.

Interestingly, of the pollen tube bursting events captured during imaging of *VTC2* OE pollen, the majority (17 out of 18 bursting events) occurred during the two growth patterns that showed abnormal Ca^{2+} signaling, oscillatory or arrested growth (Supplemental Movies S1 and S2, respectively). No bursting events were observed during the imaging of WT (0 out of 12 tubes) (Supplemental Figure S3). Thus, there is a strong association between a bursting event in a growing pollen tube and those tubes showing a *VTC2*-dependent disruption in Ca^{2+} oscillations. As pollen tube bursting is ultimately driven by an imbalance between cytosolic turgor pressure and cell wall strength, it is not clear if abnormal Ca^{2+} signals are the symptom or cause of a potential deficiency in cell wall integrity.

Models for *VTC2* OE leading to reduced pollen fertility

There are at least two models to explain how overexpression of *VTC2* might interfere with pollen fertility. The first model is dependent on increased ascorbate, where too much ROS quenching might disrupt signals required for pollen grain germination and tube growth, as speculated by Muhlemann et al. (2018). Similarly, an excess of apoplastic ascorbate could promote cell wall loosening (Green and Fry, 2005), a possible explanation for the high bursting frequency in *VTC2* OE pollen. Under severe oxidative stress, ascorbate breakdown to oxalic acid (Fenech et al., 2021) can result in the formation of oxalate–Ca^{2+} crystals in the apoplast and vacuoles, possibly affecting the pools of free Ca^{2+} (Truffault et al., 2017). However, the failure to detect an increase in ascorbate or changes in ROS favors the consideration of alternative models. For example, *VTC2* OE could alter the flux of metabolites through interconnected pathways and thereby perturb the supply of related sugar nucleotides that are critical to pathways involved in cell wall biosynthesis, such as GDP-L-galactose or GDP-D-mannose.

In support of an alternative model where *VTC2* OE might disrupt interconnected pathways, a greater than 2-fold decrease in mRNA abundance was observed for *GMP*, a key gene encoding an upstream pyrophosphorylase that catalyzes the synthesis of GDP-D-mannose (Figure 7A). Similarly, in tomatoes, mRNA abundance for *SlGMP1* was decreased in an analysis of floral buds during anthesis from *VTC2* OE lines (Deslous et al., 2021). Here in Arabidopsis, a greater than 1.5-fold reduction was also observed in mRNA abundance for *GME*, a gene encoding an upstream

epimerase that converts GDP-D-mannose to GDP-L-galactose (Figure 7B). As the feedback mechanism(s) responsible for these gene expression changes are not known, future studies are needed to determine whether the *VTC2*-dependent reduction in *GMP* or *GME* is initiated by increased *VTC2* mRNA, protein levels, or enzymatic activity of VTC2, or through metabolic feedback pathways resulting from the increased abundance of L-Gal-1-P. Despite this knowledge gap, it appears that *VTC2* overexpression in both tomato and Arabidopsis shares similar feedback pathways that could impact other biosynthetic pathways, including carbohydrate modifications associated with the cell wall, glycolipids, or glycoproteins (Lukowitz et al., 2001; Mounet-Gilbert et al., 2016; Tao et al., 2018).

Together, these results provide evidence that *VTC2* OE in Arabidopsis pollen results in severe male fertility defects, despite a failure to provide detectable increases in pollen grain ascorbate concentrations or alterations to ROS homeostasis. This favors a model in which *VTC2* OE triggered a deficiency in one or more metabolic pathways related to the biosynthesis of cell wall components, glycolipids, or glycoproteins. These deficiencies ultimately result in an inability to properly coordinate the dynamic interplay between turgor-driven pollen tube growth and maintaining cell wall integrity. Regardless of the specific deficiencies, this study demonstrates that *VTC2* OE potentiates pollen bursting, abnormal tube morphologies, and changes in growth-associated Ca^{2+} signaling.

Materials and methods

Plant materials and growth conditions

Plant expression vectors were transformed into Arabidopsis (*A. thaliana*) Col-0 using *Agrobacterium tumefaciens* (GV3101 strain) floral dip method (Clough and Bent, 1998). Sterilized seeds were sown on square Petri dishes containing 0.5× Murashige and Skoog medium (Phytotechnology Laboratories, pH 5.7), 0.05% (w/v) MES, 25 mg/L hygromycin B (Gold Biotechnology), and 1% (w/v) agar. After stratification in the dark for 48–72 h at 4°C, seeds were transferred to room temperature conditions with constant light for 10 days. Thereafter, seedlings were transplanted into soil prepared according to manufacturer guidelines (Sunshine SMB-238 SunGro Horticulture, Marathon pesticide, Cleary Turf and Ornamental Systemic Fungicide). Plants were grown to maturity in growth chambers at 22°C with 70% humidity and 16-h light (~125 μmol m^{-2} s^{-1}) followed by 8-h dark.

Plasmid construction

All plant expression constructs were made through standard molecular techniques using a pGreenII vector system (Hellens et al., 2000) with a hygromycin resistant (Hyg^R) selection marker for plants and a kanamycin-resistant (Kan^R) selection marker for *Escherichia coli*. For *VTC2* overexpression, all constructs used the promoter region from *Ca^{2+}-dependent protein kinase 34* (*CPK34p*). Plasmid stock (ps3059) included *CPK34p::VTC2* and *CPK34p::ERmCherry*; ps3217, *CPK34p::VTC2* and *Ubiquitin 10 (UBQ10) promoter::mCherry-roGFP2;* ps3202, *CPK34p::VTC2*, and *UBQ10::CGf*. Reporter constructs without *VTC2* were ps2935, *UBQ10p::CGf* (Weigand et al., 2021); ps3260, *UBQ10p::ER-CGf*; and ps3209, *UBQ10p::mCherry-roGFP2*. See Supplemental Figures S4–S8 for plasmid maps and DNA sequences.

Genetics and seed set analyses

Transgene transmission was measured by scoring hygromycin resistance of F1 progeny from selfed plants and reciprocal outcrosses. Statistical significance was determined using Pearson's chi-squared test (χ^2) unless stated otherwise. Seed set analyses were conducted using mature siliques decolorized in 70% (v/v) ethanol at room temperature over 24 h.

In vitro pollen germination

Using 1- to 2-day-old flowers, Arabidopsis pollen grains were germinated on the surface of agar containing 1.5% (w/v) low melting agarose and pollen growth media (PGM) modified from Boavida and McCormick (2007): 10% (w/v) sucrose, 2 mM Ca^{2+} chloride ($CaCl_2$), 650 μM (0.004% w/v) boric acid (H_3BO_3), 2 mM potassium chloride (KCl), 0.4 mM magnesium sulfate ($MgSO_4$), and buffered to pH 7.5 using potassium hydroxide (KOH). A humidity chamber was used to germinate pollen grains in the dark at 22°C. Pollen were incubated for various periods of time depending on the analysis. Glass coverslips were placed over pollen tubes on the agar surface prior to imaging.

Germination frequency and pollen tube length

After incubating for 10 h, pollen samples were imaged using a Keyence BZ-X700 microscope under bright-field illumination using a 20×/0.45NA air objective. Germination frequency and pollen tube length were quantified using ImageJ software (Abràmoff et al., 2004) including multi-measure and cell counter plugins.

Pollen collection for mRNA expression and ascorbate analyses

To isolate pollen, open flowers were cut and vortexed for 30 s in a 50-mL centrifuge tube containing water, followed by filtration through a 70-μm nylon mesh (Becton Dickinson and Company). Filtered pollen was pelleted at 4°C by centrifugation for 5 min at 12,000 × *g*. The supernatant was discarded. For mRNA expression analyses, lysis buffer (RLT) containing beta-mercaptoethanol (Qiagen) was added to pollen pellets per the manufacturer's guidelines. For ascorbate analyses, fresh weight was recorded. Thereafter, pollen pellets were frozen in liquid nitrogen and stored at −80°C.

RNA isolation, cDNA synthesis, and expression analyses

Total RNA was extracted from pollen samples using Qiagen RNeasy Plant Mini Kit including an optional cleaning step using RNase-free DNase (Qiagen) to eliminate genomic DNA contamination. Complementary DNA (cDNA) was synthesized using 150 ng of total RNA via BioRad iScript cDNA Synthesis Kit (BioRad Cat#1708890). RT-qPCR analyses were performed using BioRad SsoAdvanced Universal SYBR Green supermix (Cat#1725271). PCR conditions were as follows: initial denaturation 95°C for 30 s, followed by repeating cycles of 95°C for 10 s, 58°C for 20 s for 40 total cycles. Reference gene *Cyclin P2; 1* (AT3G21870) was chosen based on minimal variation in pollen expression (Rahmati Ishka et al., 2018). A fold change was calculated for *VTC2* (normalized to *CYCP2; 1*) in relation to the expression of the WT control. RT-qPCR fold changes were calculated using the delta–delta Ct (ΔΔCt) method. Primer sequences are available in Supplemental Figure S1.

Ascorbate measurement

Following pollen harvest, 60% (v/v) ice-cold methanol containing 250 μM Diethylenetriaminepentaacetic acid (DTPA, Sigma Cas#67-43-6) was added to frozen pollen pellets. Cells were mechanically lysed by bead beating for 5 min at 4°C. After lysis, 1 volume of chloroform was added for a final methanol:water:chloroform ratio of 4:3:1, respectively. Samples were vortexed and centrifuged for 10 min at 10,000 × *g*. The supernatant was transferred to a new tube and stored at −80°C.

The assay was essentially performed as described in Vislisel et al. (2007). Assay buffer containing 2 M sodium acetate adjusted to pH 5.5 with glacial acetic acid was chelated using Chelex 100 (Sigma Cas#11139-85-8) according to the manufacturer's guidelines. Individual stocks of 2.32 mM Tempol (Sigma Cas#2226-96-2) and 5.5 mM *o*-Phenylenediamine (OPDA, Sigma Cas#65-54-5) were prepared in assay buffer. Ascorbate standards were prepared in 60% (v/v) methanol containing 250 μm DTPA as a series of 1:2 serial dilutions (100, 50, 25, 12.5, and 6.25 μM L-ascorbate) (Sigma Cas#50-81-7). In triplicate, 50 μL of standards and 1:5 sample dilutions were added to individual wells of a 96-well microtiter plate (ThermoFisher cat#9205). Using a multichannel, repeat pipettor, 50-μL Tempol was added. After a 10-min incubation, 21 μL OPDA was added in a dimly lit room. After a final 10-min incubation, fluorescence was measured at excitation 345 nm and emission 425 nm using Spectramax M5 plate reader and SoftMax Pro software. Ascorbate levels were determined by interpolating fluorescent values from standard curves with R^2 value > 0.998. Due to the instability of ascorbate and light sensitivity of OPDA, the metabolite extraction, ascorbate standards, and OPDA were prepared on the day of analysis.

ROS analysis

To measure ROS accumulation, 1- to 2-day-old flowers were vortexed in 1 mL PGM (no agar). Flowers were removed using forceps, while the remaining pollen germinated in PGM for 10 min. About 1 μL of 5 mM H_2DCFDA (DCF) was added to germinating pollen solution for a final concentration of 5 μM DCF. After a 20-min incubation, pollen was pelleted by centrifugation for 5 min at 10,000 × *g*. Then, 5 μL of pelleted pollen was transferred to an agar slide. A coverslip was placed on the top of pollen grains on the agar surface. Pollen was imaged under bright-field, mCherry excitation 561 nm/emission 615 nm (to identify transgenic pollen), and yellow fluorescent protein (YFP) excitation 500 nm/emission 530 nm (DCF stain) using Keyence BZ-X700 microscope with a 20×/0.45NA air objective. YFP fluorescent intensity was measured using ImageJ multi-measure plugin. ROS accumulation was determined by normalizing fluorescent intensity to WT (non-transgenic) pollen.

To measure redox status, pollen was dusted onto individual 27-mm glass bottom dish (Thomas Scientific cat#1190X48) sprayed with medical adhesive, followed by the addition of 500 μL liquid PGM. Pollen germinated for 2 h at 22°C prior to imaging pollen using a Leica STELLARIS Spectral Point Scanner HyD S Inverted Confocal Microscope system at 20×/0.75 NA. *ro*GFP2 redox state was determined by imaging for the relative intensity of the 520 nm emission peak resulting from an excitation at either 405 nm (higher in the oxidized state) or 488 nm (higher in the reduced state). Fluorescent intensity was measured using ImageJ multi-measure plugin.

Ca^{2+} and growth time series analysis

Pollen was germinated on agar slides as described in in vitro pollen germination. Pollen time-lapse images were captured using a Leica DMi8 inverted microscope fitted with a Yokogawa CSU-W1 spinning disk confocal scanner module and a CCD camera. Images were captured with 63×/1.4 NA objective with filter switching between GFP (excitation 488 nm, intensity 100 mW, exposure 250 ms, collection bandwidth 500–550 nm, gain 250) and RFP (excitation 561 nm, intensity 150 mW, exposure 250 ms, collection bandwidth 572.5–647.5 nm, gain 250). Only pollen tubes between 100 and 400 μm in length were used for the analysis.

Using ImageJ, the region of interest for tip-focused imaging was 10 μm (pollen apex). Multiple Kymograph plugin was used to generate kymographs (average pixel neighborhood = 5) for individual fluorescent channels. Kymograph text files were analyzed using the CHUKNORRIS web interface (https://feijolab.shinyapps.io/CHUK/) for single-channel kymographs (Damineli et al., 2017). Fluorescent intensity and growth rate patterns were obtained from CHUKNORRIS output. A raw ratio (CGf ratio) was calculated from CHUKNORRIS-derived time series (ROI.ts) data to normalize Ca^{2+} signals (GCaMP6f; GFP fluorescence) to protein abundance (mCherry; RFP fluorescence).

Accession numbers

Sequence data from this article can be found in the GenBank/EMBL data libraries under the following accession

numbers: *VTC1; GMP* (At2g39770), *VTC2* (At4g26850), and *GME* (At5g28840).

Supplemental data

The following materials are available in the online version of this article.

Supplemental Figure S1. *VTC2* and *CPK34* expression profile comparison and primers used for mRNA expression analyses.

Supplemental Figure S2. *Ubiquitin10promoter::ER-CGf* does not alter reproduction.

Supplemental Figure S3. Bursting frequency of pollen tubes during steady growth (SGC), oscillatory growth (OGC), or arrested growth calcium (AGC) oscillations.

Supplemental Figure S4. ps3059 *CPK34p::VTC2* and *CPK34p::ER_mCherry* plasmid map and DNA sequence.

Supplemental Figure S5. ps3217 *CPK34p::VTC2* and *UBQ10p::mCherry-roGFP2* plasmid map and DNA sequence.

Supplemental Figure S6. ps3202 *CPK34p::VTC2* and *UBQ10p::CGf* plasmid map and DNA sequence.

Supplemental Figure S7. ps3260 *UBQ10p::ER_CGf* plasmid map and DNA sequence.

Supplemental Figure S8. ps3209 *UBQ10p::mCherry-roGFP2* plasmid map and DNA sequence.

Supplemental Movie S1. *VTC2* OE pollen tube bursting during OGC oscillations.

Supplemental Movie S2. *VTC2* OE pollen tube bursting during AGC oscillations.

Funding

This work was supported by grants to J.F.H. from NSF IOS 1656774 and IOS 2129234, G.M. and J.F.H. from BARD IS-4652-13, and G.M. from BSF 2016605. Imaging performed using Leica STELLARIS Spectral Point Scanner HyD S Inverted Confocal Microscope was supported by a grant from the National Institute of General Medical Sciences P20GM130459.

Conflict of interest statement. None declared.

References

Abràmoff MD, Magalhães PJ, Ram SJ. (2004) Image processing with imageJ. Biophotonics Int **11**: 36–41. doi:10.1201/9781420005615.ax4

Boavida LC, McCormick S (2007) Temperature as a determinant factor for increased and reproducible in vitro pollen germination in *Arabidopsis thaliana*. Plant J **52**(3): 570–582

Bulley S, Wright M, Rommens C, Yan H, Rassam M, Lin-Wang K, Andre C, Brewster D, Karunairetnam S, Allan AC, et al. (2012) Enhancing ascorbate in fruits and tubers through over-expression of the L-galactose pathway gene GDP-L-galactose phosphorylase. Plant Biotechnol J **10**(4): 390–397

Clough SJ, Bent AF (1998) Floral dip: a simplified method for Agrobacterium-mediated transformation of Arabidopsis thaliana. Plant J **16**: 735–743. doi:10.1046/j.1365-313X.1998.00343.x

Damineli DSC, Portes MT, Feijó JA (2017) Oscillatory signatures underlie growth regimes in Arabidopsis pollen tubes: computational methods to estimate tip location, periodicity, and synchronization in growing cells. J Exp Bot **68**(12): 3267–3281

Deslous P, Bournonville C, Decros G, Okabe Y, Mauxion JP, Jorly J, Gadin S, Brès C, Mori K, Ferrand C, et al. (2021) Overproduction of ascorbic acid impairs pollen fertility in tomato. J Exp Bot **72**(8): 3091–3107

Fenech M, Amaya I, Valpuesta V, Botella MA (2019) Vitamin C content in fruits: biosynthesis and regulation. Front Plant Sci **9**(January): 1–21

Fenech M, Amorim-Silva V, del Valle AE, Arnaud D, Ruiz-Lopez N, Castillo AG, Smirnoff N, Botella MA (2021) The role of GDP-L-galactose phosphorylase in the control of ascorbate biosynthesis. Plant Physiol **185**(4): 1574–1594

Foyer CH, Noctor G (2011) Ascorbate and glutathione: the heart of the redox hub. Plant Physiol **155**(1): 2–18

Frietsch S, Wang YF, Sladek C, Poulsen LR, Romanowsky SM, Schroeder JI, Harper JF (2007) A cyclic nucleotide-gated channel is essential for polarized tip growth of pollen. Proc Natl Acad Sci U S A **104**(36): 14531–14536

Gallie DR (2012) The role of L-ascorbic acid recycling in responding to environmental stress and in promoting plant growth. J Exp Bot **64**(2): 433–443

Gao Y, Badejo AA, Shibata H, Sawa Y, Maruta T, Shigeoka S, Page M, Smirnoff N, Ishikawa T (2011) Expression analysis of the VTC2 and VTC5 genes encoding GDP-L-galactose phosphorylase, an enzyme involved in ascorbate biosynthesis, in *Arabidopsis thaliana*. Biosci Biotechnol Biochem **75**(9): 1783–1788

Green MA, Fry SC (2005) Apoplastic degradation of ascorbate: novel enzymes and metabolites permeating the plant cell wall. Plant Biosyst **139**(1): 2–7

Hasanuzzaman M, Borhannuddin Bhuyan MHM, Anee TI, Parvin K, Nahar K, Al Mahmud J, Fujita M (2019) Regulation of ascorbate-glutathione pathway in mitigating oxidative damage in plants under abiotic stress. Antioxidants **8**(9): 384

Hellens RP, Anne Edwards E, Leyland NR, Bean S, Mullineaux PM (2000) pGreen: a versatile and flexible binary Ti vector for Agrobacterium-mediated plant transformation. Plant Mol Bio **42**: 819–832. doi:10.1023/A:1006496308160

Johnson MA, Harper JF, Palanivelu R (2019) A fruitful journey: pollen tube navigation from germination to fertilization. Annu Rev Plant Biol **70**(1): 809–837

Kerchev PI, Van Breusegem F (2022) Improving oxidative stress resilience in plants. Plant J **109**(2): 359–372

Laing WA, Martínez-Sánchez M, Wright MA, Bulley SM, Brewster D, Dare AP, Rassam M, Wang D, Storey R, Macknight RC, et al. (2015) An upstream open reading frame is essential for feedback regulation of ascorbate biosynthesis in Arabidopsis. Plant Cell **27**(3): 772–786

Laxa M, Liebthal M, Telman W, Chibani K, Dietz KJ (2019) The role of the plant antioxidant system in drought tolerance. Antioxidants **8**(4): 94

Lukowitz W, Nickle TC, Meinke DW, Last RL, Conklin PL, Somerville CR (2001) Arabidopsis cyt1 mutants are deficient in a mannose-1-phosphate guanylyltransferase and point to a requirement of N-linked glycosylation for cellulose biosynthesis. Proc Natl Acad Sci U S A **98**(5): 2262–2267

Luria G, Rutley N, Lazar I, Harper JF, Miller G (2019) Direct analysis of pollen fitness by flow cytometry: implications for pollen response to stress. Plant J **98**(5): 942–952

Mittler R (2017) ROS are good. Trends Plant Sci **22**(1): 11–19

Mounet-Gilbert L, Dumont M, Ferrand C, Bournonville C, Monier A, Jorly J, Lemaire-Chamley M, Mori K, Atienza I, Hernould M, et al. (2016) Two tomato GDP-D-mannose epimerase isoforms involved in ascorbate biosynthesis play specific roles in cell wall biosynthesis and development. J Exp Bot **67**(15): 4767–4777

Muhlemann JK, Younts TLB, Muday GK (2018) Flavonols control pollen tube growth and integrity by regulating ROS homeostasis during high-temperature stress. Proc Natl Acad Sci U S A **115**(47): E11188–E11197

Müller-Moulé P (2008) An expression analysis of the ascorbate biosynthesis enzyme VTC2. Plant Mol Biol **68**(1-2): 31–41

Qi T, Liu Z, Fan M, Chen Y, Tian H, Wu D, Gao H, Ren C, Song S, Xie D (2017) GDP-D-mannose epimerase regulates male gametophyte development, plant growth and leaf senescence in Arabidopsis. Sci Rep **7**(1): 1–13

Rahmati Ishka M, Brown M, Weigand E, Tillett C, Schlauch KA, Miller G, Harper JF (2018) A comparison of heat-stress transcriptome changes between wild-type Arabidopsis pollen and a heat-sensitive mutant harboring a knockout of cyclic nucleotide-gated cation channel 16 (cngc16). BMC Genomics **19**(1): 1–19

Shao HB, Chu LY, Lu ZH, Kang CM (2008) Primary antioxidant free radical scavenging and redox signaling pathways in higher plant cells. Int J Biol Sci **4**(1): 8–14

Smirnoff N (2018) Ascorbic acid metabolism and functions: a comparison of plants and mammals. Free Radic Biol Med **122**(March): 116–129

Tao J, Wu H, Li Z, Huang C, Xu X (2018) Molecular evolution of GDP-D-mannose epimerase (GME), a key gene in plant ascorbic acid biosynthesis. Front Plant Sci **9**(September): 1–10

Truffault V, Fry SC, Stevens RG, Gautier H (2017) Ascorbate degradation in tomato leads to accumulation of oxalate, threonate and oxalyl threonate. Plant J **89**(5): 996–1008

Tunc-Ozdemir M, Tang C, Ishka MR, Brown E, Groves NR, Myers CT, Rato C, Poulsen LR, McDowell S, Miller G, et al. (2013) A cyclic nucleotide-gated channel (CNGC16) in pollen is critical for stress tolerance in pollen reproductive development. Plant Physiol **161**(2): 1010–1020

Ugalde JM, Fecker L, Schwarzländer M, Müller-Schüssele SJ, Meyer AJ (2020). Live monitoring of ROS-induced cytosolic redox changes with roGFP2-based sensorsin plants. Preprint at https://www.biorxiv.org/content/10.1101/2020.12.21.423768v1. 1–33. Retrieved from https://www.biorxiv.org/content/10.1101/2020.12.21.423768v1

Vislisel JM, Schafer FQ, Buettner GR (2007) A simple and sensitive assay for ascorbate using a plate reader. Anal Biochem **365**(1): 31–39

Wang L, Meng X, Yang D, Ma N, Wang G, Meng Q (2014) Overexpression of tomato GDP-L-galactose phosphorylase gene in tobacco improves tolerance to chilling stress. Plant Cell Rep **33**(9): 1441–1451

Weigand C, Harper J (2020) Decapitation crosses to test pollen fertility mutations for defects in stigma-style penetration. Methods Mol Biol **2160**: 29–40. doi:10.1007/978-1-0716-0672-8_3

Weigand C, Kim SH, Brown E, Medina E, Mares M, Miller G, Harper JF, Choi WG (2021) A ratiometric calcium reporter CGf reveals calcium dynamics both in the single cell and whole plant levels under heat stress. Front Plant Sci **12**(December): 1–14

Yoshimura, K., Nakane, T., Kume, S., Shiomi, Y., Maruta, T., Ishikawa, T., Shigeoka, S. (2014). Transient expression analysis revealed the importance of VTC_2 expression level in light/dark regulation of ascorbate biosynthesis in Arabidopsis. Biosci Biotechnol Biochem **78**(1): 60–66

Zhang H, Xiang Y, He N, Liu X, Liu H, Fang L, Zhang F, Sun X, Zhang D, Li X, et al. (2020) Enhanced vitamin C production mediated by an ABA-induced PTP-like nucleotidase improves plant drought tolerance in Arabidopsis and maize. Mol Plant **13**(5): 760–776